Thin Solid Films, *193/194* (1990) 201–210

ON THE MICROSTRUCTURE–PROPERTY RELATIONSHIP OF W–Ti–(N) DIFFUSION BARRIERS

A. G. DIRKS, R. A. M. WOLTERS AND A. J. M. NELLISSEN
Philips Research Laboratories, 5600 JA Eindhoven (The Netherlands)

In advanced silicon technology, tungsten-rich W–Ti alloy films are frequently used as diffusion barriers and etch-stop layers in combination with aluminium-based interconnections. We have studied both microstructure and properties of magnetron sputtered $W_{80}Ti_{20}$ (atomic per cent) alloy films with and without nitrogen incorporated in the film structure. The efficiency of these films as a barrier layer has been studied by the interaction between interconnecting Al–(alloy) and W–Ti–(N) using the following samples: Al–(Cu,Si)/W–Ti–(N)/SiO_2/Si. The barrier films have been characterized with the help of cross-sectional transmission electron microscopy, electron diffraction, electrical resistivity probing, Rutherford back-scattering spectrometry and X-ray diffraction.

The $W_{80}Ti_{20}$ films exhibit a columnar microstructure. As the recrystallization temperature of these (refractory) barrier metals is far above the anneal temperature of 450 °C, the columnar growth morphology is preserved on annealing. The intercolumnar material (or low density network) provides favourite sites for vacancy condensation and forms short-circuit diffusion paths in a direction perpendicular to the plane of the films. Such $W_{80}Ti_{20}$ films therefore behave as rather poor diffusion barriers. As shown in the literature by several researchers, both the incorporation of nitrogen into the structure of W–Ti films and the application of a thin oxide film at the barrier–interconnect interface may improve the barrier properties considerably. The present investigations of the film properties resulted in a better understanding of the barrier function of both binary W–Ti and ternary W–Ti–N alloy films.

1. INTRODUCTION

Since it became feasible to use tungsten-rich W–Ti alloy films as a diffusion barrier between aluminium and the substrate in integrated circuit metallization systems[1], a large volume of data has been published. This includes work on binary W–Ti alloy films[2–5], on ternary W–Ti–N alloy films[6–13], and on interfacial oxides[14–16].

On the basis of both the modified zone model of Thornton[17] and the grain size measurements on $W_{70}Ti_{30}$ (atomic per cent) films of Nowicki *et al.*[6], Hoffman[3]

0040-6090/90/$3.50

proposed a structural model in which a 150 nm $W_{70}Ti_{30}$ film was porous with holes reaching from the substrate to surface. The 150 nm long, tapered $W_{70}Ti_{30}$ grains touch one another near the surface of the barrier film. From transmission electron microscopy (TEM) studies, Nowicki *et al.*[6] concluded that 30 nm thick W–Ti films have grain sizes in the range 10–100 nm depending on the deposition conditions. In their description of the microstructure of 150 nm thick W–Ti films Berger *et al.*[12] described the barrier layer to consist of more or less equiaxed grains with diameters in the range 30–50 nm. A rather realistic report on the $W_{70}Ti_{30}$ microstructure was presented by Oparowski *et al.*[11], who describe the binary W–Ti films as a mixture of columnar grains and fine crystals and the ternary W–Ti–N alloy films as an assembly of predominantly fine crystallites.

The process of preparing cross-sectional TEM samples by ion milling so that the microstructure of these films can be investigated is laborious and time consuming. This is due to the relative low sputter rate of refractory metal barrier films, as compared with materials such as silicon or aluminium. With a new type of ion milling equipment[18] we have succeeded in the preparation of electron-transparent regions in TEM cross-sectional samples of both binary W–Ti and ternary W–Ti–N films. The relationship between the observed microstructural phenomena and measured properties of the investigated thin barrier films will be described.

2. EXPERIMENTAL DETAILS

All metallic films were deposited onto thermally oxidized silicon wafers; the SiO_2 thickness was 0.6 μm. The W–Ti barrier films were made by d.c. magnetron sputtering with argon gas from an alloy target of composition $W_{70}Ti_{30}$ (all compositions are given in atomic per cent). However, the composition of the deposits was analysed to be $W_{80}Ti_{20}$ by Rutherford backscattering spectrometry (RBS). This may be explained by scattering of titanium atoms in the gas phase during deposition (on the sputter shields of the deposition chamber distinct titanium enrichments have been observed). The barrier film thickness was 0.07, 0.1 or 0.5 μm. The ternary W–Ti–N films were deposited by reactive sputtering in $Ar–N_2$ gas mixtures. By exposing the W–Ti–(N) layer to atmosphere a thin layer of surface oxide was grown. Next, a 0.5 μm thick film of aluminium, $Al_{99}Si_1$, or $Al_{98}Cu_1Si_1$ was deposited by magnetron sputtering.

The procedure for the preparation of TEM cross-sectional samples was as follows: after cutting two pieces of size 0.5 mm × 1.8 mm out of a silicon wafer, these pieces were fixed face-to-face inside an aluminium disc of 3 mm diameter and thickness 0.5 mm. This assembly was ground and polished on both sides to a thickness of 50 μm. The final thinning of the samples was performed using the ion milling equipment described in refs. 18 and 19. The thinning conditions are as follows: voltage, 10 kV; specimen current, 40 μA; two argon ion beams; angle of ion beam incidence (measured from the film plane), as low as $1–2^0$; thinning rate, 5–6 μm h^{-1}. The microstructural data have been supplemented with X-ray diffraction (XRD) data, electrical resistivity measurements by a four-point probing technique, and RBS.

3. RESULTS

The TEM cross-section of an as-deposited $W_{80}Ti_{20}$ film of 70 nm thickness is shown in Fig. 1(a). A schematic view is given in Fig. 1(b). The appearance of a columnar nature in the film is accentuated by the numerous voids which decorate the column "boundaries". In a previous paper[20] we have described the columnar arrangement in terms of a low density (or void) network that surrounds an array of rods of higher density. The average column size is of the order of 10 nm. In equilibrium, the $W_{80}Ti_{20}$ film is essentially a two-phase alloy with very limited mutual solid solubility. In the as-deposited situation the tungsten matrix may be supersaturated to a certain extent. Throughout the microstructure the excess titanium atoms precipitate in the form of particles, 1–10 nm in size, or as ultrafine (subnanometre) particles. RBS measurements showed that approximately 1 at.% Ar has been incorporated in the W–Ti structure. This gas content in the films is far too low to contribute substantially to the formation of voids as shown in Fig. 1. Another interesting observation is the existence of conglomerates of columns having nearly

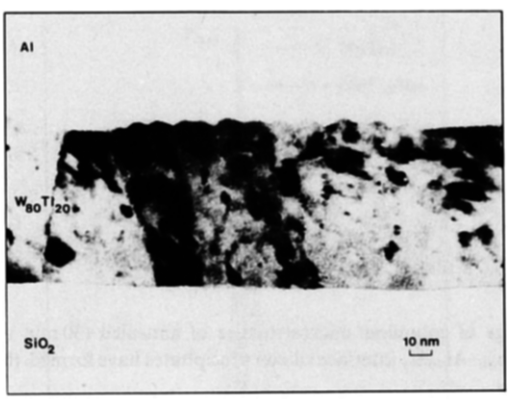

(a)

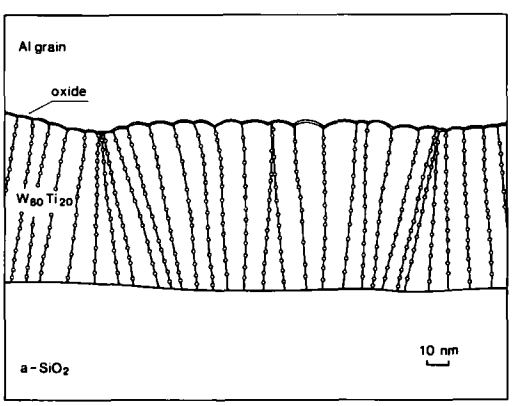

(b)

Fig. 1. Columnar microstructure of as-deposited, 70 nm thick $W_{80}Ti_{20}$ film; (a) cross-sectional TEM image; (b) schematic.

(a)

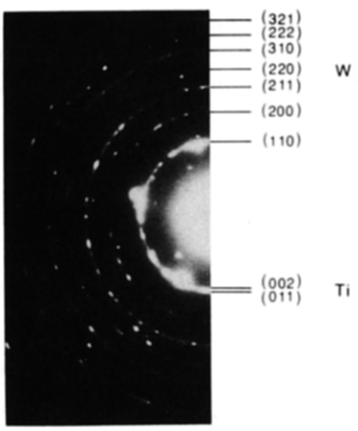

(b)

Fig. 2. Cross-sectional TEM (dark field) image of columnar microstructure of annealed (30 min at 450 °C) 0.5 μm thick $W_{80}Ti_{20}$ film. At the $W_{80}Ti_{20}$–$Al_{99}Si_1$ interface silicon precipitates have formed. (b) Electron diffraction pattern of binary W–Ti film.

the same crystal orientation. Such conglomerates may comprise some tens to some hundreds of individual columns.

In Fig. 2 a dark field TEM image is given for a 0.5 μm thick $W_{80}Ti_{20}$ film annealed for 30 min at 450 °C. The columnar microstructure has been preserved during this anneal treatment, whereas the phase separation into the equilibrium phases β-W and α-Ti becomes more pronounced on annealing. Furthermore, the microstructural details relate to the film thickness: by comparing Figs. 1 and 2 it is clear that the average column diameter increases with film thickness, *i.e.* 10 nm diameter for 70 nm thick films and 30–50 nm diameter in the 0.5 μm case. Apparently, during film growth certain columns increase their widths at the expense of others. Finally, Fig. 2(a) shows some silicon precipitates formed at the $W_{80}Ti_{20}$–$Al_{99}Si_1$ interface on annealing at 450 °C. In Fig. 2(b) the indexed electron diffraction pattern of the two-phase $W_{80}Ti_{20}$ barrier film is given.

A good example of the poor barrier properties of such a columnar-like

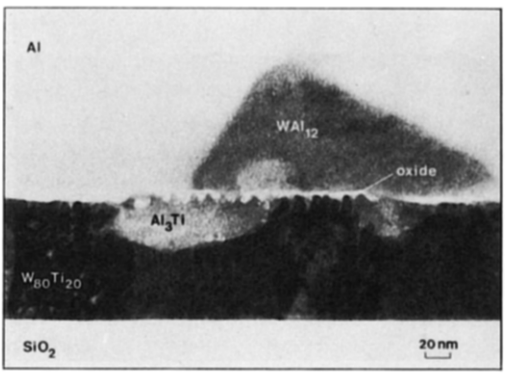

Fig. 3. Reaction products of both WAl_{12} and Al_3Ti, formed on annealing at 475 °C. The upper side of the columns at the $W_{80}Ti_{20}$–Al interface had been decorated with a thin oxide film before annealing (white region).

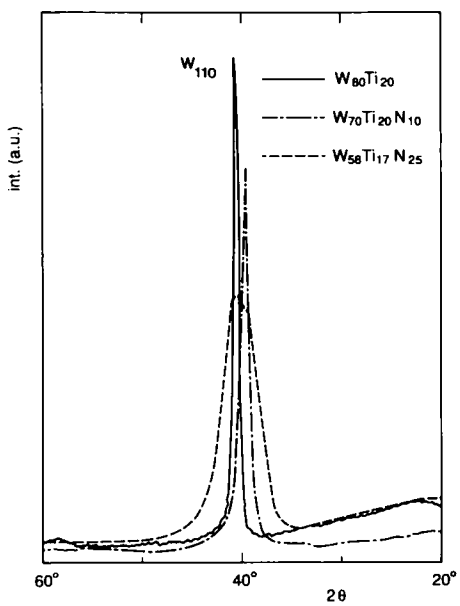

Fig. 4. XRD pattern for W–Ti–(N) alloy films as a function of the Bragg angle θ as measured with Cu Kα radiation. The pronounced (110) texture of the tungsten-rich films is reduced as the nitrogen content of the films is increased.

microstructure is presented in Fig. 3. Despite the presence of an interfacial oxide between barrier and (pure) aluminium film, compound formation has been observed after annealing up to temperatures of 475 °C. Tungsten atoms diffuse upwards along the column boundaries to form WAl_{12}, whereas aluminium atoms diffuse downwards into the W–Ti and form Al_3Ti. In addition, with both RBS measurements and TEM investigations we have observed that tungsten atoms have diffused along the

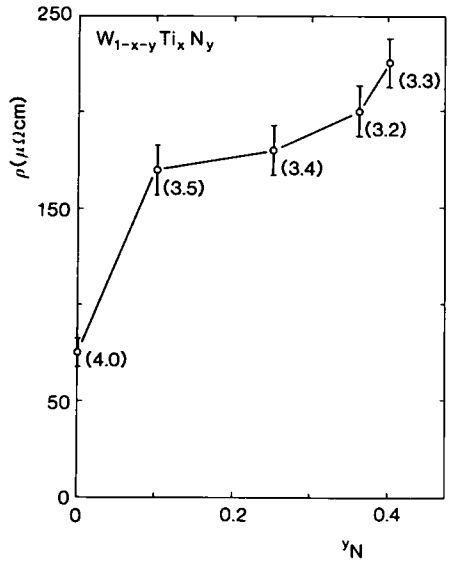

Fig. 5. Electrical resistivity ρ of as-deposited $W_{1-x-y}Ti_xN_y$ alloy films as a function of nitrogen fraction, y_N. The W:Ti ratios of the films are given by the numerals in parentheses.

aluminium grain boundaries to form tungsten-containing deposits on top of the pure aluminium film.

The barrier properties of W–Ti films can be successfully improved by the incorporation of nitrogen atoms in the barrier film[6–13]. In Fig. 4 the XRD data are given for W–Ti films which have been reactively sputtered in Ar–N_2 gas mixtures. It can be seen that the intensity of the strong W_{110} peak decreases as the nitrogen content of the films increases. Commonly, line broadening is attributed to small crystallite sizes and lattice strains, amongst other causes. Consequently, the observed decrease in average particle size may not be the only reason for line broadening. In addition, the pronounced shift in the θ value of the W_{110} peak is indicative of the complex character of the phase changes which occur when the nitrogen content of the films increases. The RBS measurements on the W–Ti–N films reveal a decrease in the W:Ti ratio with increasing nitrogen content. Supplementary measurements of the electrical resistivity ρ of as-deposited ternary alloy films are presented in Fig. 5. A dramatic increase in ρ is found with increasing nitrogen content of the films. Electron scattering at the enormous volume of phase boundaries (see Fig. 6), the saturation of the matrix with nitrogen and the formation of (a number of) nitride phases may all contribute to this observed increase in ρ. In Fig. 5 the W:Ti ratio is given by the numerals in parentheses. On annealing for 30 min at 450 °C, changes in ρ of the order of only 5% have been observed. As just indicated, a considerable change in the microstructural morphology was also observed when nitrogen was added to the W–Ti alloy films. On comparing the TEM cross-section of binary $W_{80}Ti_{20}$ (Fig. 1(a)) with that of ternary $W_{58}Ti_{17}N_{25}$ (Fig. 6(a)), it may be concluded that the columnar nature seems to be less manifest in

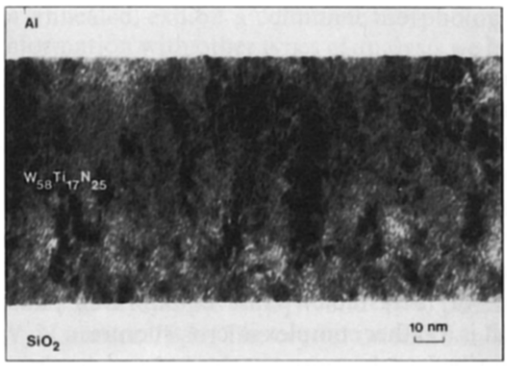

(a)

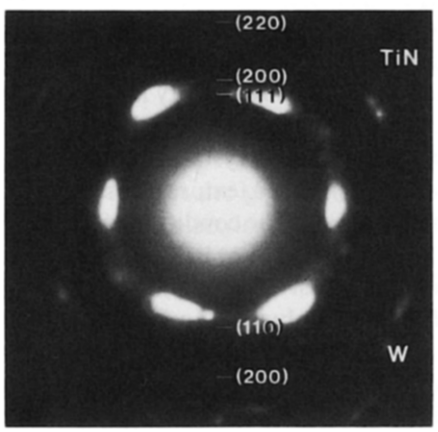

(b)

Fig. 6. (a) Cross-sectional TEM image of 83 nm thick $W_{58}Ti_{17}N_{25}$ alloy film after a 30 min anneal at 450 C; (b) electron diffraction pattern of ternary W–Ti–N alloy film.

the nitrogen-containing films. Dark field images, however, still exhibit the columnar-like morphology. Within each column the β-W matrix is broken up into an intimate mixture of small crystallites with dimensions of 1–2 nm. Both this overall precipitation and the absence of voiding guarantee a much denser microstructure in the ternary W–Ti–N alloy films as compared with binary W–Ti alloys. In addition, the electron diffraction pattern in Fig. 6(b) strongly suggests the presence of the TiN phase. This cubic nitride is highly textured and its orientation seems to be related to the (110) planes of the β-W matrix. As well as the TiN and β-W phases, small crystallites of W_2N and/or Ti_2N may be present. Obviously, it is an over-simplification to describe the improved barrier properties of W–Ti–N films in terms of "stuffing the grain boundaries with nitrogen". The ternary W–Ti–N alloy films exhibit, in combination with aluminium, excellent diffusion barrier properties[8]. Heating such samples in an N_2–H_2 gas ambient for 30 min at 450 °C (or even 500 °C) did not result in any appreciable change in interfacial structure.

4. DISCUSSION

Deposition of atoms onto substrates under the condition of "limited atomic mobility" commonly results in the formation of columnar structures[20]. In thin films of refractory metals, such as (pure) tungsten, this microstructure has been reported for both magnetron-sputtered[21–23] and chemically vapour deposited[24] thin films. The column dimensions in these films are thickness dependent, *i.e.* the columns increase their average diameter as they grow[21]. Also, in multiphase alloy films, either crystalline or amorphous, columnar microstructures have frequently been observed[20]. In order to arrive at a stable (or metastable) phase equilibrium, phase separation has to occur. Often the result is a rather complex microstructure.

W–Ti alloy films have been described to be porous membranes[3], to have equiaxed grains[12], or to exhibit lamella-type structures[4]. On the contrary, the present results agree in broad outline with the observations of Oparowski *et al.*, who report on columnar grains and fine crystallites[11]. Our investigations indicate the presence of a significant number of small voids within the low density network. The columns themselves consist of a β-W matrix seeded with fine α-Ti precipitates. The formation of conglomerates of columns with the same crystal orientation, as described in Section 3, may be explained in terms of enforced texture during growth by a certain column in the centre of such a conglomerate. The condition of a limited atomic mobility is a prerequisite in this case.

In ternary W–Ti–N alloy films (containing at least 25 at.% N) the columnar morphology of the films is still present, although less obvious. In fact, the rather strong texture of the cubic TiN phase, orientation related to the β-W matrix of each individual column, maintains the continuing columnar nature of the films. These multiphase W–Ti–N alloy films may also be described as a dense mixture of ultrafine crystallites of β-W and TiN, possibly together with the phases W_2N and Ti_2N. This complexity of the microstructure is reflected in the huge increase of electrical resistivity of the films with increasing nitrogen content.

During the 450 °C anneal of W–Ti/Al–(alloy) combinations, the atomic mobility of both tungsten atoms and aluminium atoms is high, especially along the void-decorated low density network. Here tungsten atoms diffuse towards the interconnect and form WAl_{12}, while aluminium atoms diffuse into the barrier and form Al_3Ti. In ternary W–Ti–N barrier films the situation is quite different: both tungsten and titanium atoms are already immobilized during the deposition by the formation of nitrides. In addition, void formation is rather unlikely during the nucleation and growth process of such a large number of extremely small crystallites. This may explain the enhanced barrier properties of ternary W–Ti–N alloy films as compared with the W–Ti binaries. A study of the changes in the microstructural phenomena as induced by a variation in the nitrogen content of the films is in progress.

5. CONCLUSIONS

With cross-sectional TEM we have resolved some microstructural details of both binary W–Ti and ternary W–Ti–N alloy films. All films, whether as deposited

or annealed, exhibit a columnar morphology. By combination of the microscopic information with other types of analysis we have come to the following conclusions.

(1) Binary $W_{80}Ti_{20}$ alloy films are composed of a two-phase structure of a β-W matrix seeded with fine α-Ti precipitates. The low density network surrounding the columns is decorated by voids, thus providing short-circuit diffusion paths in a direction perpendicular to the film plane. Despite the application of a thin oxide film at the $W_{80}Ti_{20}$–Al interface, the formation of compounds, such as WAl_{12} and Al_3Ti, has been observed on annealing at 475 °C.

(2) Ternary $W_{58}Ti_{17}N_{25}$ alloy films may be described as a dense mixture of ultrafine crystallites of β-W and TiN, possibly together with small crystallites of W_2N and/or Ti_2N. The crystal orientation of the TiN phase is related to the (110) orientation of the β-W matrix of each individual column. The intimate phase separation in combination with the nitride formation observed result in a substantial improvement in the barrier properties of these ternary films, compared with binary $W_{80}Ti_{20}$ films.

ACKNOWLEDGMENTS

The authors are grateful to E. P. Naburgh and E. T. Swart for both sputter deposition and electrical resistivity measurements, to M. F. C. Willemsen for RBS measurements, and to A. G. Mouwen-Tijssen for XRD experiments.

REFERENCES

1 J. A. Cunningham, C. R. Fuller and C. T. Haywood. *IEEE Trans. Reliab.*, *19* (1970) 182.
2 P. B. Ghate, J. C. Blair, C. R. Fuller and G. E. McGuire, *Thin Solid Films*, *53* (1978) 117.
3 V. Hoffman, *Solid State Technol.*, *26* (June 1983) 119.
4 C. J. Palmstrøm, J. W. Mayer, B. Cunningham, D. R. Campbell and P. A. Totta, *J. Appl. Phys.*, *58* (1985) 3444.
5 P.-H. Chang, H.-Y. Liu, J. A. Keenan, J. M. Anthony and J. G. Bohlman, *J. Appl. Phys.*, *62* (1987) 2485.
6 R. S. Nowicki, J. M. Harris, M.-A. Nicolet and I. V. Mitchell, *Thin Solid Films*, *53* (1978) 195.
7 A. Joshi, L. D. Hartsough and D. R. Denison, *Thin Solid Films*, *64* (1979) 409.
8 R. A. M. Wolters and A. J. M. Nellissen, *Solid State Technol.*, *29* (February 1986) 131.
9 D. Gloesener, G. Puylaert and F. Van de Wiele, *Vide, Couches Minces*, *42* (1987) 175.
10 J. M. Oparowski, R. D. Sisson and R. R. Biederman, *Thin Solid Films*, *153* (1987) 313.
11 J. M. Oparowski, D. F. Quaranta, R. R. Biederman and R. D. Sisson, *Microstruct. Sci.*, *16* (1988) 379.
12 S. Berger, Y. Komem and I. Blech, *Thin Solid Films*, *176* (1989) 131.
13 I. J. M. M. Raaijmakers, *Proc. Annu. Meet. of the Mining, Metallurgy and Materials Society, Anaheim, CA, February 1990*, to be published.
14 C. Canali, F. Fantini, G. Queirolo, and E. Zanoni, *Proc. 19th IEEE Int. Reliability Symp.*, IEEE, New York, 1981, p. 230.
15 C. Canali, G. Celotti, F. Fantini and E. Zanoni, *Thin Solid Films*, *88* (1982) 9.
16 J. O. Olowolafe, C. J. Palmstrøm, E. G. Colgan and J. W. Mayer, *J. Appl. Phys.*, *58* (1985) 3440.
17 J. A. Thornton, *J. Vac. Sci. Technol.*, *11* (1974) 666.
18 Á. Barna, in Á. Csanády, P. Roehlich and D. Szabo (eds.), *Proc. 8th Eur. Conf. on Electron Microscopy, Budapest, 1984*, p. 107.
19 Á. Barna and P. B. Barna, *Proc. 3rd Balkan Conf. on Electron Microscopy, Athens, 1989*, to be published.

20 A. G. Dirks and H. J. Leamy, *Thin Solid Films*, *47* (1977) 219.
21 D. Goyal and A. H. King, in J. Sanchez, D. A. Smith and N. DeLanerolle (eds.), *Microstructural Science for Thin Film Metallization in Electronics Applications*, Minerals, Metals and Materials Society, Warrendale, PA, 1988, p. 139.
22 M. G. Hugon, F. Varniere, B. Agius, M. Froment, C. Arena and J. Bessot, *Appl. Surf. Sci.*, *38* (1989) 269.
23 A. M. Haghiri-Gosnet, F. R. Ladan, C. Mayeux and H. Launois, *J. Vac. Sci. Technol. A*, *7* (1989) 2663.
24 S. R. Herd, K. Y. Ahn, P. M. Fryer and J. M. Karasinski, in R. S. Blewer and C. M. McConica (eds.), *Workshop on Tungsten and Other Refractory Metals for VLSI Applications IV, Albuquerque, NM*, Materials Research Society, Pittsburgh, PA, 1989, p. 47.